ANTIOXIDANTS & REDOX SIGNALING
Volume 12, Number 2, 2010

DOI: 10.1089/ars.2009.2798

Differential Induction of Renal Heme Oxygenase and Ferritin in Ascorbate and Nonascorbate Producing Species Transfused with Modified Cell-Free Hemoglobin

Omer I. Butt,[1] Paul W. Buehler,[1] and Felice D'Agnillo

Abstract

Heme catabolism and iron sequestration systems play an important role in regulating the response to extracellular hemoglobin (Hb). We previously reported that extracellular Hb oxidizes more readily in the circulation of guinea pigs, a nonascorbate (AA)-producing species with similar plasma and tissue antioxidant status to humans, compared to rats, an AA-producing species. To determine whether these two species exhibit differences in heme catabolism and iron sequestration at the level of the kidney, we examined heme oxygenase (HO), H- and L-ferritin expression, nonheme iron deposition, and renal AA content following transfusion with polymerized bovine hemoglobin (HbG). Both species showed similar rates of hemoglobinuria but urinary HbG was significantly more oxidized in guinea pigs. HbG enhanced HO activity in both species but appeared greater and more sustained in guinea pigs. Conversely, rats showed a greater and more rapid induction of H- and L-ferritin as well as greater iron accumulation and AA content. Furthermore, ferrous and ferric iron deposits were detected in rats while only ferric iron was observed in guinea pigs. These findings suggest significant differences in the renal handling of HbG which may be important for understanding how endogenous antioxidant defenses may modulate the renal response to extracellular Hb. *Antioxid. Redox Signal.* 12, 199–208.

Introduction

Hemoglobin (Hb) is normally sequestered inside erythrocytes where antioxidant enzymes such as superoxide dismutase, catalase, and low molecular weight molecules such as glutathione and ascorbate (AA) maintain its oxygen-carrying reduced state (ferrous, Fe^{2+}). Hb released by hemolysis or used in the development of oxygen therapeutics can oxidize to produce methemoglobin (ferric, Fe^{3+}), ferryl heme intermediate (Fe^{4+}), hemichromes, and free heme or iron (3). Redox reactions driven by Hb or its breakdown products may ultimately trigger oxidative damage in the vasculature and tissues although the mechanisms are not completely understood. Intravascular and tissue reductive and heme catabolic systems that can limit the progression of Hb-catalyzed oxidative damage but, under certain settings, these protective mechanisms may be overwhelmed (3, 5).

We previously proposed that studying animal species with similar antioxidant profiles to humans could provide useful insight on the mechanisms of Hb-mediated cardiovascular dysfunction or injury (7, 9). Guinea pigs, like humans, cannot synthesize their own AA while rats are efficient producers of AA (21). In addition to AA, guinea pigs and humans share other similarities with respect to tissue antioxidant capabilities. For example, copper and zinc superoxide dismutase (SOD) enzymatic activity in kidney and liver is approximately twofold higher in humans and guinea pigs compared to rats (21). The efficiency of ascorbate recycling in the human and guinea pig red blood cell is also similar and differs to that of the rat (27). Thus, the overall antioxidant status of guinea pig and human are quite similar, such that the balance of reductive capacity is tilted toward the tissue and away from the plasma in these species.

Heme oxygenase (HO) is the rate-limiting enzyme of heme catabolism. Inducible HO-1 and constitutive HO-2 catalyze the degradation of heme to biliverdin, an intermediate in the production of bilirubin, free iron, and carbon monoxide (1). HO-1 is upregulated by heme, hypoxia, heavy metals, and

Laboratory of Biochemistry and Vascular Biology, Division of Hematology, Center for Biologics Evaluation and Research, Food and Drug Administration, Bethesda, Maryland.
[1]These authors contributed equally.
The findings and conclusions in this article have not been formally disseminated by the Food and Drug Administration and should not be construed to represent any Agency determination or policy.

other stimuli (1). Kidney HO activity is normally very low but increases dramatically following exposure to filtered heme proteins and/or heme resulting from hemolysis, rhabdomyolysis, or the infusion of hemoglobin oxygen therapeutics (1, 11, 22, 23, 26, 33). Filtered hemoglobin is either taken up by proximal tubules via megalin and cubilin receptors or excreted in the urine when levels exceed reabsorption capacity (10). HO-1 upregulation is often accompanied by ferritin induction as a mechanism to trap liberated iron and limit oxidative stress (2, 4, 5, 20). Ferritin is composed of 24 subunits of ferritin heavy (H-ferritin, 21 kDa) and light (L-ferritin, 19 kDa) chains in ratios that vary in different tissues and under different cellular stresses. Ferritin synthesis is primarily regulated post-transcriptionally by a process that involves an iron-binding regulatory protein (IRP) that senses the intracellular concentration of iron (12, 30). Transcriptional regulation of ferritin by oxidative stress has also been described (12).

Previous studies suggest that the redox state of Hb or iron can modulate HO and ferritin (4, 20, 24, 29). For example, HO and ferritin expression in rat lung was increased by infusion of ferric Hb but not ferrous Hb (4). Others have suggested that efficient induction of ferritin in iron-overloaded guinea pigs is stimulated by Fe^{2+} maintained through ascorbate reductive processes (24). We previously reported that polymerized bovine hemoglobin (HbG) oxidized more readily in the circulation of guinea pigs than in rats and this correlated with decreased intravascular levels of AA in guinea pigs (9). In light of these previous findings, we hypothesized that rats and guinea pigs could exhibit differences in heme catabolic and iron sequestration responses to extracellular Hb. Using a 50% exchange transfusion (ET) model, we examined the effect of HbG on renal heme oxygenase (HO), H- and L-ferritin expression, nonheme ferrous and ferric iron deposition, and renal AA content in rats and guinea pigs. The rationale for selecting a 50% ET was based on previous observations (9), and further confirmed herein, that this model does not produce significant renal toxicity in either species. Our results indicate that rats and guinea pigs differ in their induction of HO and ferritin, the nature and accumulation of nonheme iron, and renal AA content. Given the similarities in antioxidant status between guinea pigs and humans, these findings may have implications for understanding the pathophysiology of Hb in hemolytic disease states and with the administration of Hb therapeutics to individuals with diminished antioxidant defenses.

Materials and Methods

Materials

Oxyglobin® (hemoglobin glutamer–200 bovine, HbG), a product approved for veterinary use, was purchased from Biopure Corporation (Cambridge, MA). This solution consists of a heterogeneous mixture of glutaraldehyde polymerized bovine hemoglobin at a concentration of 13 g/dL in modified lactated Ringer's. The solution contains unstabilized tetramers (<5%), stabilized 64 kDa tetramers (~35%), 65–130 kDa oligomers (~50%), and 500 kDa polymers (<10%). Detailed physiochemical characterization has been previously reported (8). The initial content of HbG in the ferric form was 5.7%. All other chemicals were obtained from Sigma (St. Louis, MO) unless indicated otherwise.

Antibodies

Rabbit polyclonal HO-1 (SPA-894) and HO-2 (OSA-200) antibodies and a horseradish peroxidase (HRP)-conjugated goat anti-rabbit secondary antibody (SAB300) were obtained from Assay Designs (Victoria, BC). Goat polyclonal ferritin light chain (L-ferritin, sc-14422) and rabbit polyclonal ferritin heavy chain (H-ferritin, sc-25617) antibodies, and HRP-conjugated donkey anti-goat and goat anti-rabbit antibodies were obtained from Santa Cruz Biotechnology (Santa Cruz, CA).

Animals and surgical preparation

Male Sprague–Dawley rats and Hartley guinea pigs were purchased from Charles Rivers Laboratories (Wilmington, MA) and acclimated for 1 week upon arrival to the FDA/Center for Biologics Evaluation and Research (CBER) animal care facility. All animals were fed normal diets throughout the acclimation period and weighed 350–450 g at the time of study. Animal protocols for each species were approved by the FDA/CBER Institutional Animal Care and Use Committee with all experimental procedures performed in adherence to the National Institutes of Health guidelines on the use of experimental animals. Catheterization of the right common carotid artery and the left external jugular vein was performed as previously described (9).

Experimental protocol

Fully conscious and freely moving rats and guinea pigs underwent a 50% exchange transfusion (ET) replacing blood with HbG, as previously reported (9). Rats and guinea pigs received 3122 ± 55 and 3272 ± 106 mg/kg doses of HbG, respectively, which produced end-ET maximum plasma HbG concentrations of 4.2 ± 0.2 and 4.0 ± 0.2 g/dL, respectively (9). The half life of HbG under these experimental conditions was calculated as 15.6 and 15.7 h in rats and guinea pigs, respectively. Sham control animals underwent the surgical procedure and were allowed to recover for 24 h prior to sacrifice. At the indicated times, the animals were anesthetized, the femoral veins were cut, and cold saline was perfused via the arterial catheter to remove blood. Kidneys were dissected, cut in half, and frozen immediately in liquid nitrogen and stored at -80°C or fixed in 10% formalin. Both species typically excreted urine containing HbG within a 2 h period after the start of ET. Urine samples were collected over this time period, centrifuged, and stored at -80°C prior to analysis.

Plasma creatinine analysis

Plasma samples were filtered through 10 kDa cutoff filter units prior to analysis to eliminate Hb assay interference. Creatinine was measured in the filtrate using a Beckman Coulter LX-20 analyzer (Fullerton, CA).

HbG redox state and stability

Spectral analysis of HbG in urine samples was performed using a rapid scanning diode array spectrophotometer (Model HP-8453, Agilent Technologies, Rockville, MD). The concentrations of HbG in the ferrous, ferric, and hemichrome forms were determined using multi-component analysis as previously reported (34). Size exclusion chromatography

(SEC) and MALDI-MS to determine HbG molecular size distribution and globin chain presence in urine were performed as previously described for plasma (9).

HO activity measurement

Renal microsomes were prepared by ultracentrifugation, as previously described (16, 18). Microsomal membranes (0.5–1 mg/ml) were added to reaction mixtures containing glucose 6-phosphate (2 m*M*), glucose-6-phosphate dehydrogenase (1.6 U/ml), hemin (15 μM), 0.5 mg of rat liver cytosol prepared from a 105,000 g supernatant fraction as a source of biliverdin reductase, in potassium phosphate buffer (PBS, 100 m*M*, pH 7.4) containing $MgCl_2$ (0.2 m*M*). After adding NADP (0.8 m*M*) to the experimental tube and assay buffer to the reference tube, the mixtures were incubated for 1 h at 37°C in the dark. The tubes were then placed on ice for 2 min and subsequently analyzed using a scanning spectrophotometer (Perkin Elmer Lambda 18, Waltham, MA). Bilirubin was calculated by the difference in absorbance between 464 and 530 nm (40 mM^{-1} cm^{-1}). Heme oxygenase activity was expressed as nanomoles of bilirubin produced per hour per mg protein. Protein content was determined using the BCA protein assay (Pierce, Rockford, IL).

Western blot analyses

Kidney tissue (100–200 mg) that included both cortical and medullary sections from a cross-sectional cut through the center of the kidney were homogenized in ice cold lysis buffer (50 m*M* Tris, pH 7.6, 150 m*M* NaCl, 1% IgePal-630, 1 m*M* EDTA, 0.25% sodium deoxycholate) containing protease inhibitors (Cocktail Set III, Calbiochem, CA). Homogenates were incubated for 30 min on ice and then centrifuged at 15,000 g for 30 min. Supernatants were divided into aliquots and stored at −80°C. Protein concentration was measured by the BCA method. Samples were run on Bis-Tris 4%–12% polyacrylamide gels, transferred to polyvinylidene fluoride (PVDF) membranes, and blocked in Tris-buffered saline with 0.1% Tween 20 (TBS-T) containing 5% nonfat dry milk. Membranes were incubated with primary antibodies to HO-1 (1:5,000), HO-2 (1:2,500), H-ferritin (1:1,000), and L-ferritin (1:1,000) in TBS-T with 1% nonfat dry milk. After multiple washes in TBS-T, the membranes were incubated with relevant HRP-conjugated secondary antibodies in TBS-T with 1% nonfat dry milk. Detection was carried out using the ECL Plus chemiluminescence kit (Amersham, Arlington Heights, IL). Densitometry analysis was performed using NIH ImageJ software. Equal protein loading was verified by stripping and reprobing membranes for β-actin.

Nonheme iron histochemistry with DAB intensification

Nonheme Fe^{3+} and Fe^{2+} were detected using the Perls and Turnbull method, respectively, followed by DAB intensification (19). Paraffin-embedded kidney sections were de-waxed in xylene and rehydrated in graded ethanol and deionized water. Sections were incubated with equal volumes of 5% potassium ferrocyanide (Perls) or potassium ferricyanide (Turnbull) and 2% HCl for 45 min at room temperature and then rinsed in deionized water. Sections were then incubated with 0.3% hydrogen peroxide and 0.01 *M* sodium azide in methanol for 30 min at room temperature. Sections were then rinsed in 0.1 *M* phosphate buffer, pH 7.4, incubated with DAB-H_2O_2 (Sigma) for 4 min, washed in deionized water, and lightly counterstained with Gill's II hematoxylin. After dehydrating in graded ethanol and xylene, slides were mounted in Permount and coverslipped. Semiquantitative analysis of Perls-DAB staining was performed using the ImageJ software (NIH, Bethesda, MD) with color deconvolution. A total of 10 random cortical fields per kidney were imaged at a magnification of 200× and evaluated using the uncalibrated optical density (OD) software function. Staining intensity was reported as the mean of uncalibrated OD ± SE for 4–7 animals per time interval. Staining was absent in negative control sections incubated with Perls or Turnbull reagent in water instead of HCl.

Renal ascorbate measurement

Frozen kidney sections were homogenized in ice-cold 0.3% metaphosphoric acid (4 vol/g tissue) containing 25 μg/ml acetaminophen as the internal standard. Homogenates were centrifuged at 16,000 g for 30 min at 4°C, and supernatants were subsequently filtered through 0.2 μm filter units. Standards containing AA and acetaminophen were prepared in homogenization buffer. Standards and samples were analyzed by HPLC as previously described (9). The ratio of AA/acetaminophen was used to calculate renal AA concentrations and was expressed as μmol AA/g tissue.

Statistical analysis

Data are represented as means ± standard error (SE) for replicate experiments. Statistical analysis was performed by ANOVA with post-hoc Student's t-test using the JMP (v. 5.1) software (SAS Institute Inc, Cary, NC). $P < 0.05$ was considered statistically significant.

Results

Plasma creatinine and hemoglobinuria following HbG transfusion

We previously reported significant differences in systemic blood pressure in guinea pigs compared to rats, and mild to moderate changes in renal histology by hematoxylin-eosin staining in both species following 50% exchange transfusion with HbG (9). Masson's Trichrome histology also indicated minimal interstitial fibrosis in either species over the course of 72 h (data not shown). To further evaluate gross renal function, we measured time-dependent changes in plasma creatinine levels. Figure 1A shows minor increases in plasma creatinine well within the normal range for both species over the course of 72 h, suggesting HbG does not produce a major change in renal function in this model. Hemoglobinuria occurred in both species within the first 2 h after the start of HbG infusion, but was generally not detectable after this initial phase. Over the initial 2 h collection period, no significant species differences were observed in urine volumes or in rates of hemoglobinuria for guinea pig (3.1 ± 1.0 mg HbG/2 h, $n = 5$) compared to rat (1.9 ± 0.4 mg HbG/2 h, $n = 4$). Together, these data suggest the renal exposure of HbG were similar between these species and the previously reported systemic blood pressure differences likely did not translate to species differences in renal artery vascular resistance/flow.

To indirectly assess the nature of HbG exposure to renal tubules, we examined the redox state and stability of HbG in urine samples. Representative images of urine samples

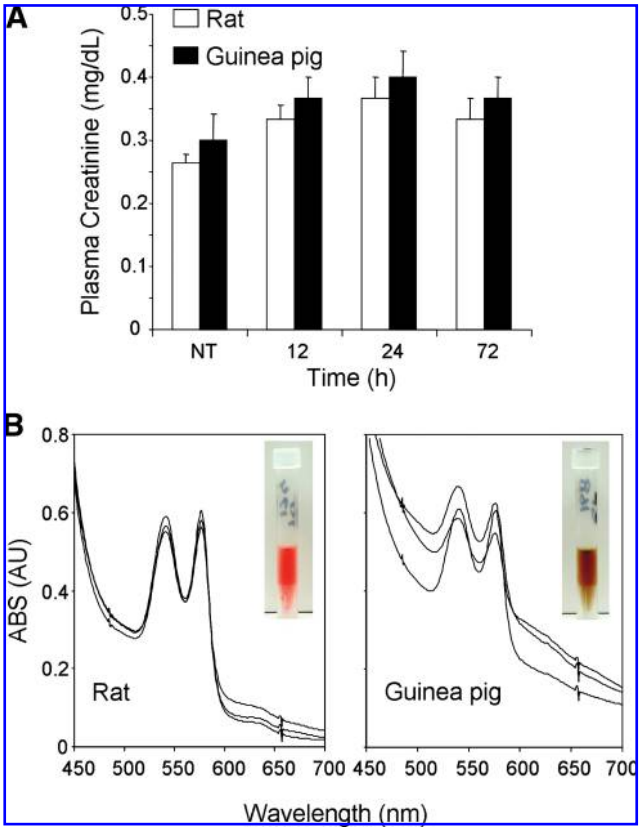

FIG. 1. Plasma creatinine and hemoglobinuria following HbG transfusion. (**A**) Plasma creatinine was measured at baseline and 12, 24, and 72 h post-ET with HbG in rats and guinea pigs. (**B**) Redox state and stability of HbG in urine. Spectral analysis (450–700 nm) of urine collected from rat (*left panel*) and guinea pig (*right panel*) after ET with HbG. Each panel shows the spectral tracings of three separate urine samples collected from three different animals. Each sample was diluted to $\sim 50\ \mu M$ (as heme) prior to analysis. Typical Hb peaks at 540 and 577 nm are clearly identifiable in both species. Absorbance increases at 630 and 700 nm in guinea pig samples are indicative of greater HbG oxidation and breakdown compared to rat. Insets show a representative image of a urine sample from rat (*red*) and guinea pig (*brown*). (For interpretation of the references to color in this figure legend, the reader is referred to the web version of this article at www.liebertonline.com/ars).

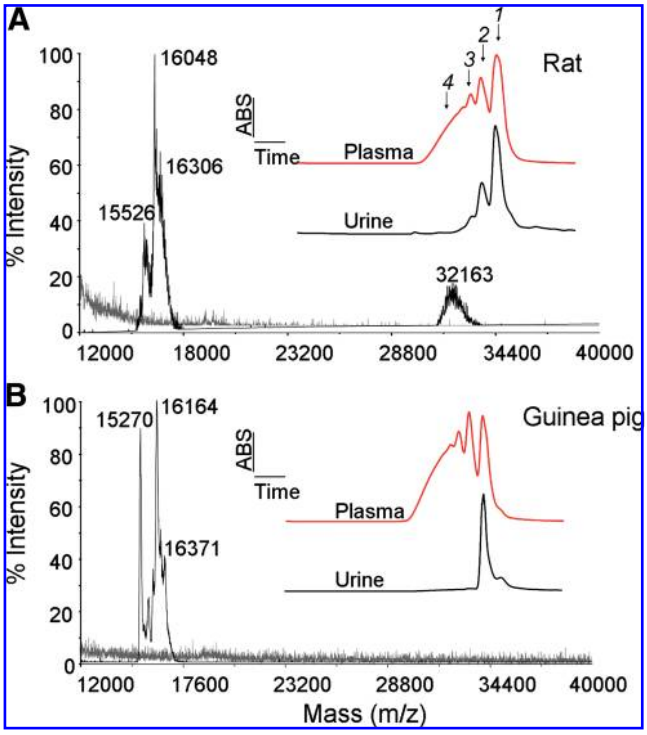

FIG. 2. MALDI-MS analysis of HbG globin chain destabilization in urine. In rat (**A**), peaks identified as α ($m/z =$ 15526.35), β (m/z = 16048.93 and 16306.93) and α–α ($m/z =$ 32163.74), denote the α, β, and α–α cross-linked species of the tetramer fraction of HbG. In guinea pig (**B**), peaks identified as α ($m/z = 15270.01$), β ($m/z = 16164.03$ and 16371.80), denote the α and β species of tetrameric HbG. The increase in intensity of the α ion could not be assigned to guinea pig red cell Hb ($m/z = 15228.59$), thus the observed intensity increase is consistent with HbG α–α cross-link destabilization. Insets show representative size exclusion chromatographs of plasma (*red line*) and urine (*black line*) samples collected at the end of ET with wavelength detection set at 405 nm. Plasma contains stabilized tetrameric as well as multimer fractions, while urine samples contain primarily stabilized tetramers. *1* (64 kDa), *2* (128 kDa), *3* (250 kDa), and *4* (>500 kDa). (For interpretation of the references to color in this figure legend, the reader is referred to the web version of this article at www.liebertonline.com/ars).

revealed a clear color distinction between HbG in guinea pig urine (brown, oxidized) versus rat urine (reddish brown) (Fig. 1B, insets). Visible spectra of guinea pig urine samples showed a greater absorbance at 630 and 700 nm compared to rat urine, indicative of greater oxidation and protein breakdown (Fig. 1B). The composition of HbG in the ferrous, ferric, and hemichrome forms in guinea pig urine was $35 \pm 7\%$, $52 \pm 7\%$, and $13 \pm 5\%$, respectively, compared to $68 \pm 3\%$, $28 \pm 3\%$, and $4 \pm 1\%$, respectively, for rat urine. These data indicate that HbG in guinea pig urine is more oxidized and/or denatured than in rat urine.

Comparative analyses of plasma and urine samples by SEC revealed that the tetrameric fraction of HbG is the predominate species excreted in both rats and guinea pigs (Fig. 2A and B, insets). However, we noted that rat urine showed some degree of variability with respect to the content of higher molecular size fractions. Some rats showed minor amounts of oligomers while others did not. In guinea pig urine, we detected a small but reproducible increase in a molecular size species smaller than the tetrameric fraction, indicative of globin chain dissociation. To assess tetramer stability in urine samples, MALDI-MS analysis was performed. In rat, cross-linked HbG derived α globin chains (α–α) were seen as an [M+H] ion ($m/z = 32163.74$), consistent with an α–α ion previously observed in HbG starting material (8). Non cross-linked α globin was observed as a low intensity [M+H] ion ($m/z = 15526.35$). The β globin chain [M+H] ion is observed at $m/z = 16048.93$. In guinea pig, no stable α–α ion was detected in urine, suggesting that filtered HbG tetramer observed in the SEC chromatogram is unstable. Further confirming this observation and contrary to rat, a high intensity HbG derived α globin chain [M+H] ion ($m/z = 15270.01$) was observed in guinea pig urine, while HbG derived β globin chains are seen

as an [M+H] ion ($m/z = 16164.03$). Consistent with increased heme iron oxidation, these data support the interpretation that cross-linked HbG tetramer excreted in the urine of guinea pig is more prone to destabilization than in rat.

Renal HO induction in HbG-transfused rats and guinea pigs

Renal HO activity was measured in HbG-transfused rats and guinea pigs over the course of 72 h. Rat HO activity increased at 4 h and peaked at 12 h (Fig. 3). Guinea pig HO activity peaked at 24 h and attained levels that were four- to fivefold greater than in rats at 12 and 24 h, respectively. In both species, HO activity returned to sham control levels by 72 h. To assess the relative contributions of HO-1 and HO-2 expression to total HO activity, Western blot analyses were performed. In rats and guinea pigs, HO-1 was upregulated at 4, 12, and 24 h compared to their respective sham controls (Fig. 4A and B). Notably, rat HO-1 expression decreased after 12 h whereas guinea pig HO-1 remained elevated between 12 and 24 h, consistent with the temporal changes in HO activity observed for both species (Fig. 3). HO-2 was not upregulated in either species (Fig. 4A and B). Immunohistochemical analysis showed that HO-1 localized predominately to renal proximal tubules in rats and guinea pigs and was not induced in glomeruli (data not shown). Overall, these data demonstrate that both rats and guinea pigs upregulate renal HO-1 expression following ET with HbG, however total HO activity appears to be higher and more sustained in guinea pigs compared to rats.

Renal ferritin expression in HbG-transfused rats and guinea pigs

To assess the ferritin response in HbG-transfused animals, the renal expression of ferritin heavy (H-ferritin) and light chain (L-ferritin) was measured by Western blot. In rats, H-ferritin expression increased by sevenfold at 4 h, remained elevated through 24 h, and declined by 72 h (Fig. 5A). Conversely, guinea pig H-ferritin expression was not upregulated over the course of 72 h (Fig. 5B). Rat L-ferritin was upregulated by about three- to fourfold and, similar to H-ferritin, significant increases were noted after 4 h. Guinea pig L-ferritin expression began to increase at 12 h and reached 3.5-fold by 72 h (Fig. 5B). These data suggest the ferritin response in HbG-treated rats is more robust, particularly in terms of H-ferritin, and occurred more rapidly than in guinea pig, which remarkably showed no H-ferritin induction.

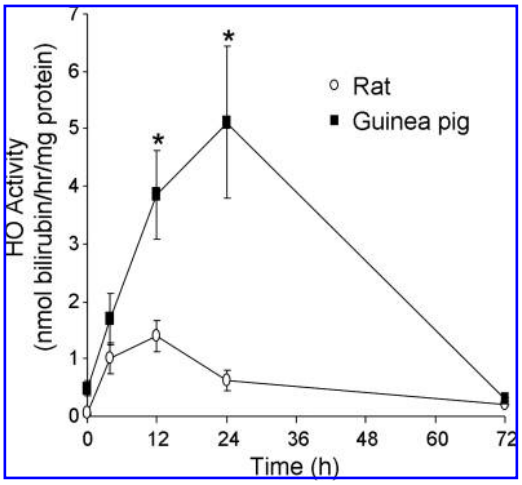

FIG. 3. Renal HO activity in Hb-transfused rats and guinea pigs. Kidneys were harvested from sham control animals (T = 0) and at 4, 12, 24, and 72 h post-ET with HbG. HO activity was measured by the bilirubin spectrophotometric assay and reported as nmol bilirubin formed/hr/mg protein. Values are shown as the means ± SEM for at least four animals per species for each time point. *$p < 0.05$ *vs.* rat at 12 and 24 h.

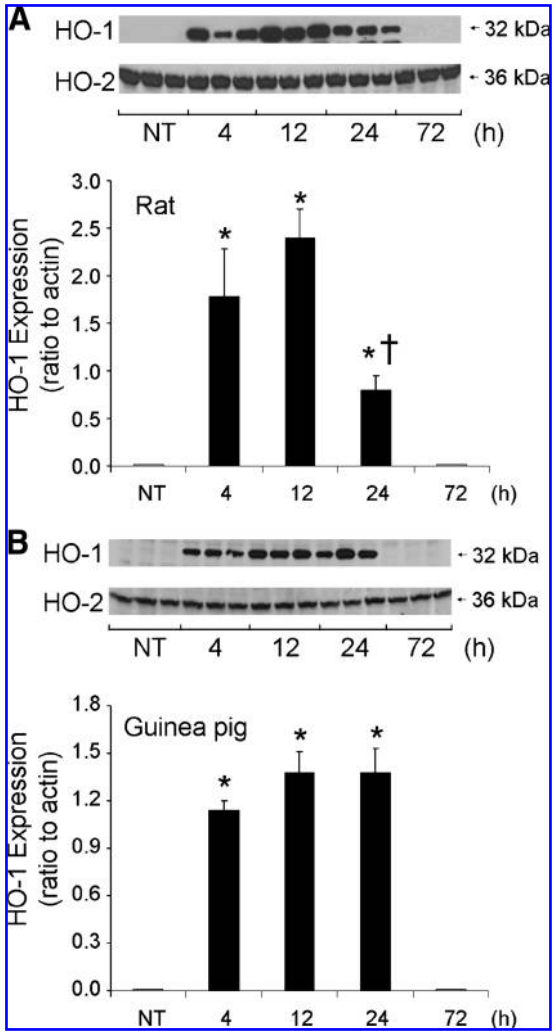

FIG. 4. Western blot analysis of renal HO-1 and HO-2 expression in rats (A) and guinea pigs (B). Kidneys were harvested from sham control animals (NT) and 4, 12, 24, and 72 h post-ET with HbG. Tissue extracts were prepared and analyzed by Western blot using a polyclonal anti-HO-1 antibody as described in the Material and Methods section. Representative immunoblots for HO-1 and HO-2 are shown for three different animals analyzed for each time point. Densitometry analysis of HO-1 expression relative to actin loading control is shown as the means ± SEM. *$p < 0.05$ *vs.* NT. †$p < 0.05$ *vs.* 12 h HO-1.

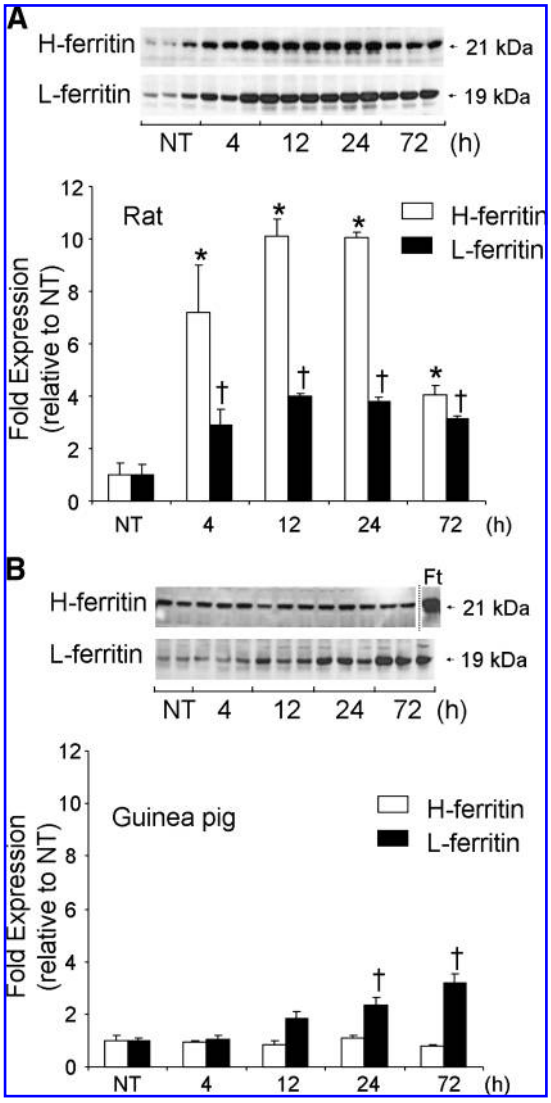

FIG. 5. Western blot analysis of ferritin heavy and light chain in rats (A) and guinea pigs (B). Kidneys were harvested from sham control animals (NT) and 4, 12, 24, and 72 h post-ET. Tissue lysates were prepared and analyzed by Western blot as described in the Material and Methods section. Representative immunoblots and corresponding densitometry for H-ferritin and L-ferritin relative to NT animals were performed for three different animals at each time point. In (**B**), the lane labeled Ft represents 50 ng of horse spleen ferritin (Sigma) run as a positive control for the anti-H-ferritin antibody. $^{*}p < 0.05$ *vs.* H-ferritin NT, $^{\dagger}p < 0.05$ *vs.* L-ferritin NT.

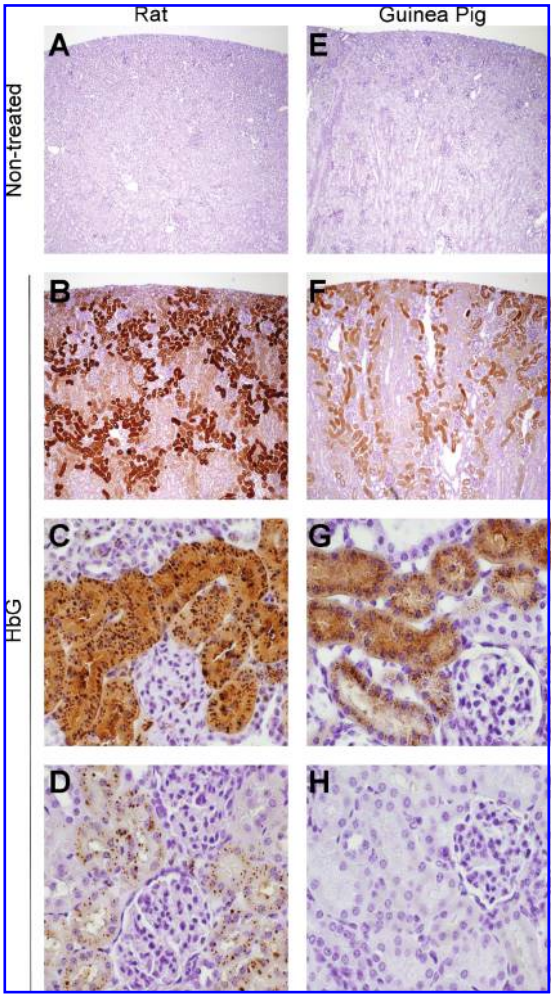

FIG. 6. Nonheme iron histochemistry using the Perls (Fe^{3+}, ferric) and Turnbull (Fe^{2+}, ferrous) methods with DAB intensification. Representative brightfield images of Perls DAB-stained kidney sections from rats (*left*) and guinea pigs (*right*) in nontreated sham control animals (**A**, **E**) and HbG-transfused animals 24 h post-ET (**B**, **F**), and 72 h post-ET (**C**, **G**). Note the relatively greater staining intensity at 24 h and the accumulation of larger and denser iron deposits in rat compared to guinea pig. Representative brightfield images of Turnbull-stained sections of HbG-transfused rats (**D**) and guinea pigs (**H**). Sections in **D** and **H** correspond to the same animals analyzed in **C** and **G**, respectively. Positive Turnbull reactivity was detectable in rats but absent in guinea pig. Magnification: ×100 (**A**, **B**, **E**, **F**) or ×400 (**C**, **D**, **G**, **H**). (For interpretation of the references to color in this figure legend, the reader is referred to the web version of this article at www.liebertonline.com/ars).

Nonheme iron accumulation in kidneys of rats and guinea pigs

To assess nonheme iron deposition, kidney sections were stained using the Perls or Turnbull method which detects Fe^{3+} or Fe^{2+}, respectively, followed by DAB intensification (19). Minimal Perls-detectable Fe^{3+} was observed in sham control rats and guinea pigs (Fig. 6A and E). Prominent Fe^{3+} deposition was observed in the proximal tubules, but not in the glomeruli or medullary regions, of HbG-transfused rats and guinea pigs (Fig. 6B and F). High magnification images revealed an increase in large iron-laden vacuolar structures, likely lysosomal hemosiderin, in rat proximal tubular cells (Fig. 6C). In contrast, less dense and smaller cytoplasmic Fe^{3+} deposits were observed in guinea pig (Fig. 6G). At 24 h post-ET with HbG, Fe^{3+} deposition was significantly greater in rats compared to guinea pigs (Fig. 7). Rat proximal tubules also showed Fe^{2+} positivity by the Turnbull method (Fig. 6D). Fe^{2+} staining in rat kidneys was most intense at 72 h while weaker or variable positivity was observed at 12 and 24 h. Conversely, in guinea pig, Fe^{2+} deposits were minimally detectable over the course of 72 h (Fig. 6H). These data indicate

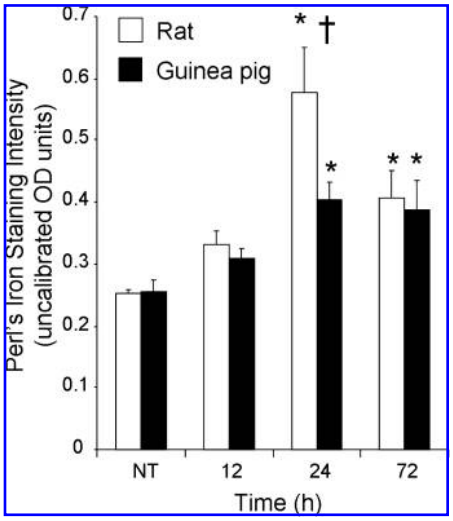

FIG. 7. Semiquantitative analysis of nonheme iron deposition. Kidney sections from sham control animals (NT) and at 12, 24, and 72 h post-ET with HbG were stained by the Perls-DAB method. Staining intensity was analyzed as described in the Materials and Methods section. *Bars* denote the means of uncalibrated OD ± SE for 10 random renal cortical images from 4–7 animals per time interval. $^{*}p < 0.05$ *vs.* NT, $^{\dagger}p < 0.05$ *vs.* 24 h guinea pig.

that nonheme iron accumulates in the kidneys of both species, but the nature of deposition differs in terms of the extent of iron accumulation, the morphological appearance of the deposits, and the presence of detectable Fe^{2+}.

Renal ascorbate content following HbG transfusion

We previously reported that plasma AA decreases by ~50% in guinea pigs, while rats maintain near normal plasma ascorbate levels after a 50% ET with HbG (9). Given the important role of intracellular AA in iron metabolism and storage pathways, we extended these earlier data by measuring renal AA levels over the course of 72 h post-ET. Figure 8 shows that renal AA was not altered significantly in HbG-transfused guinea pigs compared to sham controls. In contrast, renal AA increased significantly by 12 h in HbG-transfused rats before declining to near baseline levels by 24 and 72 h. Renal AA levels were generally greater in rats than in guinea pigs.

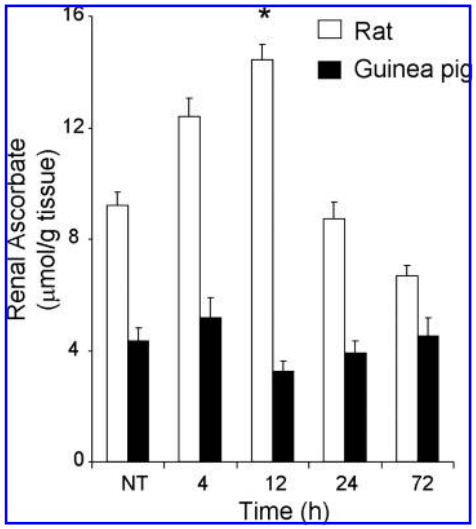

FIG. 8. Renal ascorbate content in rats and guinea pigs following ET with HbG. Tissue extracts were prepared and analyzed by HPLC as described in the Materials and Methods section. Ascorbate levels are reported as µmol/g tissue. Data are shown as the means ± SE for at least four animals per time interval. $^{*}p < 0.05$ *vs.* NT rat.

Discussion

The present study examined heme catabolism and iron sequestration in the kidney of rats (an AA-producing species) and guinea pigs (a non-AA producer) following HbG transfusion. The main findings were (a) HbG excreted by guinea pigs was found to be more oxidized (heme iron) and unstable (globin chains) than HbG excreted by rats; (b) HO enzymatic activity was increased and more sustained in guinea pig compared to rat following HbG transfusion; (c) rats showed an early induction (≤12 h) of both H- and L-ferritin while guinea pigs showed a comparatively delayed induction of L-ferritin (≥12 h) and surprisingly no induction of H-ferritin; (d) basal AA content in rat kidneys was found to be approximately twofold greater than in guinea pigs. AA levels increased transiently in rats but remained relatively constant in guinea pigs following HbG transfusion; (e) nonheme iron accumulation with detectable Fe^{2+} and Fe^{3+} deposits was greater in rats compared to guinea pigs which showed only Fe^{3+} deposits. Taken together, these data demonstrate that extracellular Hb may undergo differential renal heme breakdown and metabolism in animal species with different intravascular and tissue reductive capacities. Figure 9 summarizes the proposed processes that may be modulated by AA in this system.

Guinea pigs, unlike rats, do not synthesize AA due to the evolutionary lack of the enzyme L-gluconolactone oxidase (21). We previously showed that a 50% ET with HbG produced ~50% reduction in plasma AA in guinea pigs, whereas

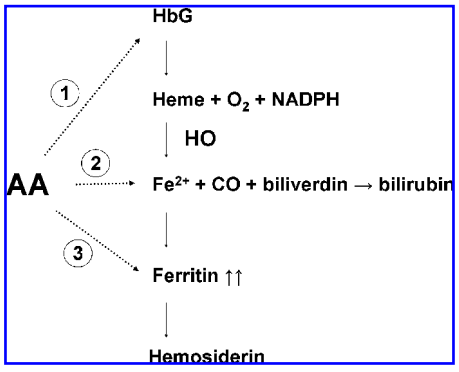

FIG. 9. Potential processes modulated by AA. 1: AA can limit the oxidation of ferrous HbG to the more unstable ferric HbG which may release heme more easily and ultimately trigger a greater HO response. **2**: Intracellular AA plays a key role in maintaining the reduced form of iron which may partly explain the increased detection of ferrous iron in kidneys of rats but not guinea pigs. Ferrous iron may also be a more potent inducer of ferritin synthesis. **3**: AA may directly influence intracellular ferritin content by directly modulating ferritin transcription and/or inhibiting ferritin degradation to hemosiderin.

plasma AA levels remained near or slightly above baseline in rats (9). Consistent with the resulting differences in plasma reducing capacities, plasma HbG was shown to oxidize more rapidly in guinea pigs. The results of the present study are similar in that urinary HbG in guinea pig showed approximately a twofold higher methemoglobin (ferric) content compared to rats. Mass spectrometry data confirmed the destabilization of HbG tetramer to globin chains in guinea pig urine, a finding that was also similar to mass spectrometry data of HbG in plasma analyzed from transfused guinea pigs (9). In this 50% ET model, the maximum plasma concentration and half-life of HbG was found to be essentially identical between these species (~4 g/dL and 15 h, respectively). This, combined with the present data showing similar HbG excretion rates between species and a lack of major renal dysfunction, suggest the total renal exposure to HbG was similar between these species. Together, these data provide indirect evidence that the renal epithelium of guinea pig was likely exposed to greater oxidized and denatured forms of HbG compared to rats. An important limitation of the present study is the absence of the direct measurement of glomerular filtration rates (GFR). Others have shown that doses of purified bovine Hb or polymerized Hb solutions similar to that used in the present study (~2–3 g/kg) produced minimal to no changes in GFR (6, 17, 26). However, to our knowledge, similar experiments have not been performed in guinea pig.

The nature of Hb exposure to renal tubular epithelium may be important with respect to renal uptake processes as Hb breakdown products such as lipid-soluble heme may gain greater access to epithelium. Previous studies have shown that hemin or ferric Hb, which releases heme more easily than ferrous Hb, are more effective inducers or substrates of HO than ferrous hemoglobin (4, 20, 29). Consistent with this idea, our finding that HbG induced a more robust HO activation in guinea pigs may be explained, at least in part, by the greater tubular exposure to oxidized and destabilized HbG. Besides the direct tubular interaction with heme, megalin- and/or cubilin-mediated endocytosis of Hb could also be an important consideration (10). However, further studies will be required to compare the nature and/or efficiency of Hb uptake mechanisms between these species and whether the redox state of Hb influences these processes.

Extensive studies by the Nath laboratory support an important role for HO in renal protection from heme damage (33). The beneficial effects are related to the removal of toxic heme as well as the generation of bile pigments and CO which together have antioxidant, antiapoptotic, vasodilatory, and anti–inflammatory properties. However, several studies have shown that HO may not always be protective or beneficial (1, 11, 14, 15, 25, 28, 35). Some studies, for example, have suggested that excess iron production by HO may aggravate or produce toxicity (15, 25, 35). In the case of heme- or heme protein-mediated stress, the protective actions of HO have consistently been linked to the simultaneous induction of ferritin (4, 5, 22, 33). The present study showed that HbG produced a near parallel induction of HO and ferritin consisting of both L- and H-chain upregulation in rats. In surprising contrast, the rapid and robust HO induction in guinea pigs was not accompanied by a corresponding ferritin response and surprisingly H-ferritin induction was absent. Moreover, in rats, when HO activity and HO-1 expression declined to baseline levels by 72 h, ferritin content also decreased significantly. In guinea pigs, however, HO returned to baseline levels by 72 h but L-ferritin expression still appeared to be increasing at this time. Our data therefore support the close association between HO and ferritin previously reported in rats but, in the case of guinea pigs, our results suggest an apparent disconnect between the extent and temporal response of HO and ferritin following HbG transfusion.

The finding that these species showed differences with respect to the type of ferritin chains expressed may be important in that each chain performs different functions. H-ferritin has potent ferroxidase activity that catalyzes the oxidation of Fe^{2+} to its Fe^{3+} storage form, whereas L-ferritin plays a role in iron nucleation and protein stability (12, 30). H-ferritin stimulation is thought to reflect an acute response to short-term iron stress while L-ferritin expression is associated with long-term iron storage and is prominent in the liver or spleen. The lack of H-ferritin induction in guinea pigs may be an indication that existing basal levels of H-ferritin and/or other iron regulating or transport mechanisms effectively limit the conditions that would trigger the need for more H-ferritin synthesis. The differential ferritin response may also be consistent with the different pattern and extent of nonheme iron accumulation observed between these species. Rat kidneys displayed large vacuolar iron deposits at 24 h which were even larger and more prevalent at 72 h. This appearance is consistent with the accumulation of lysosomal hemosiderin, the breakdown product of ferritin, and is likely a reflection of the greater amount of ferritin synthesis and degradation in rats. In the kidneys of transfused guinea pigs, iron accumulated to a lesser extent and staining generally appeared diffuse within the cytoplasm of proximal tubule cells, and small vacuolar deposits were only visible at 72 h.

Previous studies suggest that AA plays an important role in regulating ferritin synthesis and degradation (13, 24, 31, 32). Toth *et al.* showed that AA enhances ferritin translation in cells stimulated with iron (32). This enhancement was attributed to the AA-mediated conversion of free IRP to an active aconitase form (31). AA also retards degradation of ferritin by blocking lysosomal autophagy of ferritin and subsequent conversion to hemosiderin (13). In the present study, renal AA content in rats, but not guinea pigs, increased in the first 12 h and then declined to basal levels by 72 h. This temporal pattern correlated well with rat expression of L- and H-ferritin supporting a potential relationship between AA and the induction of ferritin. The finding that Fe^{2+} deposits were detected in rats but not in guinea pigs also seems consistent the presence of a greater AA reductive environment in rat kidney. Interestingly, others have suggested that Fe^{3+} may act as a poor stimulus for ferritin synthesis. Rosner *et al.* reported that AA-driven reduction of iron (Fe^{2+}) was required for efficient ferritin synthesis in iron-loaded scorbutic guinea pigs (24).

Guinea pigs and humans appear to have compensated for the lack of endogenous AA production by increasing tissue antioxidant enzyme content and efficiency (7, 9, 21). The present and previously reported findings suggest that studying animal species with similar antioxidant profile to humans may provide new insight on the mechanisms of extracellular Hb metabolism. These results may also have broader implications for understanding the catabolism of extracellular Hb by other organ systems which may be worthy of further investigation. Studies using disease state models may be warranted to evaluate how these differences in heme metabolic

processes may influence the mechanisms of Hb-induced toxicity in hemolytic disease states as well as the safety of Hb therapeutics particularly in clinical settings of depleted antioxidant status.

Acknowledgments

This work was supported by a Critical Path Initiative award from CBER/FDA.

Author Disclosure Statement

No competing financial interests exist.

References

1. Abraham NG and Kappas A. Pharmacological and clinical aspects of heme oxygenase. *Pharmacol Rev* 60: 79–127, 2008.
2. Agarwal A, Balla J, Alam J, Croatt AJ, and Nath KA. Induction of heme oxygenase in toxic renal injury: A protective role in cisplatin nephrotoxicity in the rat. *Kidney Int* 48: 1298–307, 1995.
3. Alayash AI, D'Agnillo F, and Buehler PW. First-generation blood substitutes: what have we learned? Biochemical and physiological perspectives. *Expert Opin Biol Ther* 7: 665–675, 2007.
4. Balla J, Nath KA, Balla G, Juckett MB, Jacob HS, and Vercellotti GM. Endothelial cell heme oxygenase and ferritin induction in rat lung by hemoglobin *in vivo*. *Am J Physiol* 268: L321–327, 1995.
5. Balla J, Vercellotti GM, Jeney V, Yachie A, Varga Z, Jacob HS, Eaton JW, and Balla G. Heme, heme oxygenase, and ferritin: How the vascular endothelium survives (and dies) in an iron-rich environment. *Antioxid Redox Signal* 9: 2119–2137, 2007.
6. Bonegio RG, Fuhro R, Ragno G, Robert Valeri C, and Lieberthal W. A comparison of the acute hemodynamic and delayed effects of 50% exchange transfusion with two different cross-linked hemoglobin based oxygen carrying solutions and Pentastarch. *Artif Cells Blood Substit Immobil Biotechnol* 34: 145–157, 2006.
7. Buehler PW and Alayash AI. Toxicities of hemoglobin solutions: In search of *in vitro* and *in vivo* model systems. *Transfusion* 44: 1516–1530, 2004.
8. Buehler PW, Boykins RA, Norris S, Freedberg DI, and Alayash AI. Structural and functional characterization of glutaraldehyde-polymerized bovine hemoglobin and its isolated fractions. *Anal Chem* 77: 3466–3478, 2005.
9. Buehler PW, D'Agnillo F, Hoffman V, and Alayash AI. Effects of endogenous ascorbate on oxidation, oxygenation, and toxicokinetics of cell-free modified hemoglobin after exchange transfusion in rat and guinea pig. *J Pharmacol Exp Ther* 323: 49–60, 2007.
10. Gburek J, Verroust PJ, Willnow TE, Fyfe JC, Nowacki W, Jacobsen C, Moestrup SK, and Christensen EI. Megalin and cubilin are endocytic receptors involved in renal clearance of hemoglobin. *J Am Soc Nephrol* 13: 423–430, 2002.
11. Hill-Kapturczak N and Agarwal A. Haem oxygenase-1-a culprit in vascular and renal damage? *Nephrol Dial Transplant* 22: 1495–1499, 2007.
12. Hintze KJ and Theil EC. Cellular regulation and molecular interactions of the ferritins. *Cell Mol Life Sci* 63: 591–600, 2006.
13. Hoffman KE, Yanelli K, and Bridges KR. Ascorbic acid and iron metabolism: alterations in lysosomal function. *Am J Clin Nutr* 54: 1188S–1192S, 1991.
14. Juncos JP, Grande JP, Murali N, Croatt AJ, Juncos LA, Hebbel RP, Katusic ZS, and Nath KA. Anomalous renal effects of tin protoporphyrin in a murine model of sickle cell disease. *Am J Pathol* 169: 21–31, 2006.
15. Khan ZA, Barbin YP, Cukiernik M, Adams PC, and Chakrabarti S. Heme-oxygenase-mediated iron accumulation in the liver. *Can J Physiol Pharmacol* 82: 448–456, 2004.
16. Kutty RK and Maines MD. Oxidation of heme c derivatives by purified heme oxygenase. Evidence for the presence of one molecular species of heme oxygenase in the rat liver. *J Biol Chem* 257: 9944–9952, 1982.
17. Lee R, Atsumi N, Jacobs EE Jr, Austen WG, and Vlahakes GJ. Ultrapure, stroma-free, polymerized bovine hemoglobin solution: Evaluation of renal toxicity. *J Surg Res* 47: 407–411, 1989.
18. Maines M. Carbon monoxide and nitric oxide homology: Differential modulation of heme oxygenases in brain and detection of protein and activity. *Methods Enzymol* 268: 473–488, 1996.
19. Meguro R, Asano Y, Odagiri S, Li C, Iwatsuki H, and Shoumura K. Nonheme-iron histochemistry for light and electron microscopy: A historical, theoretical and technical review. *Arch Histol Cytol* 70: 1–19, 2007.
20. Motterlini R, Foresti R, Vandegriff K, Intaglietta M, and Winslow RM. Oxidative-stress response in vascular endothelial cells exposed to acellular hemoglobin solutions. *Am J Physiol* 269: H648–655, 1995.
21. Nandi A, Mukhopadhyay CK, Ghosh MK, Chattopadhyay DJ and Chatterjee IB. Evolutionary significance of vitamin C biosynthesis in terrestrial vertebrates. *Free Radic Biol Med* 22: 1047–1054, 1997.
22. Nath KA, Balla G, Vercellotti GM, Balla J, Jacob HS, Levitt MD, and Rosenberg ME. Induction of heme oxygenase is a rapid, protective response in rhabdomyolysis in the rat. *J Clin Invest* 90: 267–270, 1992.
23. Pimstone NR, Engel P, Tenhunen R, Seitz PT, Marver HS, and Schmid R. Inducible heme oxygenase in the kidney: a model for the homeostatic control of hemoglobin catabolism. *J Clin Invest* 50: 2042–2050, 1971.
24. Roeser HP, Sizemore DJ, Nikles A, and Cham BE. Tissue ferritin in scorbutic guinea-pigs. *Br J Haematol* 55: 325–333, 1983.
25. Schipper HM. Heme oxygenase expression in human central nervous system disorders. *Free Radic Biol Med* 37: 1995–2011, 2004.
26. Somers M, Piqueras AI, Strange K, Zeidel ML, Pfaller W, Gawryl M, and Harris HW. Interactions of ultrapure bovine hemoglobin with renal epithelial cells *in vivo* and *in vitro*. *Am J Physiol* 273: F38–52, 1997.
27. Su D, May JM, Koury MJ, and Asard H. Human erythrocyte membranes contain a cytochrome b561 that may be involved in extracellular ascorbate recycling. *J Biol Chem* 281: 39852–39859, 2006.
28. Suttner DM and Dennery PA. Reversal of HO-1 related cytoprotection with increased expression is due to reactive iron. *FASEB J* 13: 1800–1809, 1999.
29. Tenhunen R, Marver HS, and Schmid R. Microsomal heme oxygenase. Characterization of the enzyme. *J Biol Chem* 244: 6388–6394, 1969.
30. Torti FM and Torti SV. Regulation of ferritin genes and protein. *Blood* 99: 3505–3516, 2002.
31. Toth I and Bridges KR. Ascorbic acid enhances ferritin mRNA translation by an IRP/aconitase switch. *J Biol Chem* 270: 19540–19544, 1995.
32. Toth I, Rogers JT, McPhee JA, Elliott SM, Abramson SL, and Bridges KR. Ascorbic acid enhances iron-induced ferritin

translation in human leukemia and hepatoma cells. *J Biol Chem* 270: 2846–2852, 1995.
33. Tracz MJ, Alam J, and Nath KA. Physiology and pathophysiology of heme: Implications for kidney disease. *J Am Soc Nephrol* 18: 414–420, 2007.
34. Winterbourn CC. *CRC Handbook of Methods of Oxygen Radical Research.* RA. Boca Raton, CRC Press, 1985, pp. 137–141.
35. Zager RA, Burkhart KM, Conrad DS, and Gmur DJ. Iron, heme oxygenase, and glutathione: Effects on myohemoglobinuric proximal tubular injury. *Kidney Int* 48: 1624–1634, 1995.

Address correspondence to:
Felice D'Agnillo, Ph.D.
Center for Biologics Evaluation and Research
Food and Drug Administration
29 Lincoln Drive, Bldg. 29, Rm. 129
Bethesda, MD, 20892

E-mail: felice.dagnillo@fda.hhs.gov

Date of first submission to ARS Central, July 29, 2009; date of acceptance, August 6, 2009.

Abbreviations Used

AA = ascorbate
BCA = bicinchoninic acid
DAB = diaminobenzidine
EDTA = ethylenediaminetetraacetic acid
ET = exchange transfusion
Hb = hemoglobin
HbG = polymerized bovine hemoglobin
HO = heme oxygenase
HRP = horseradish peroxidase
MALDI-MS = matrix-assisted laser desorption/ionization mass spectrometry
SEC = size exclusion chromatography

This article has been cited by:

1. J. H. Baek, Y. Zhou, D. R. Harris, D. J. Schaer, A. F. Palmer, P. W. Buehler. 2012. Down Selection of Polymerized Bovine Hemoglobins for Use as Oxygen Releasing Therapeutics in a Guinea Pig Model. *Toxicological Sciences* **127**:2, 567-581. [CrossRef]
2. Jin Hyen Baek, Felice D'Agnillo, Florence Vallelian, Claudia P. Pereira, Matthew C. Williams, Yiping Jia, Dominik J. Schaer, Paul W. Buehler. 2012. Hemoglobin-driven pathophysiology is an in vivo consequence of the red blood cell storage lesion that can be attenuated in guinea pigs by haptoglobin therapy. *Journal of Clinical Investigation* . [CrossRef]
3. Paul W. Buehler, Felice D'AgnilloAnimal Models and Oxidative Biomarkers to Evaluate Preclinical Safety of Extracellular Hemoglobins 391-411. [CrossRef]
4. Paul W. Buehler, Omer I. Butt, Felice D'Agnillo. 2011. Sodium nitrite induces acute central nervous system toxicity in guinea pigs exposed to systemic cell-free hemoglobin. *Biochemical and Biophysical Research Communications* **409**:3, 412-417. [CrossRef]
5. Omer I. Butt, Paul W. Buehler, Felice D'Agnillo. 2011. Blood-Brain Barrier Disruption and Oxidative Stress in Guinea Pig after Systemic Exposure to Modified Cell-Free Hemoglobin. *The American Journal of Pathology* **178**:3, 1316-1328. [CrossRef]
6. Brandon J. Reeder . 2010. The Redox Activity of Hemoglobins: From Physiologic Functions to Pathologic Mechanisms. *Antioxidants & Redox Signaling* **13**:7, 1087-1123. [Abstract] [Full Text HTML] [Full Text PDF] [Full Text PDF with Links]
7. Paul W. Buehler, Felice D'Agnillo, Dominik J. Schaer. 2010. Hemoglobin-based oxygen carriers: from mechanisms of toxicity and clearance to rational drug design. *Trends in Molecular Medicine* **16**:10, 447-457. [CrossRef]